18916

Diffraction Imaging Using Plane-wave Destructor Filters in Common-depth Specularity Gathers

I. Sturzu (Z-Terra Inc), T.J. Moser* (Moser Geophysical Services), A.M. Popovici (Z-Terra Inc), I. Musat (Z-Terra Inc) & N. Tanushev (Z-Terra Inc)

SUMMARY

Seismic diffraction imaging is recognized as a rapidly emerging technology with great potential to reduce exploration and production risks and increase recovery, for conventional reservoirs as well as unconventional resources such as shale gas. The idea behind diffraction imaging in a pre-stack migration framework is to apply a weight factor inside the migration loops, which attenuates events that satisfy Snell's law of specular reflection, while preserving diffractive events that do not satisfy Snell's law. Here we further develop an approach, called specularity gathers, to construct the weight factor in a very efficient way. We introduce a method to filter the specular energy from specularity gathers in order to obtain diffraction images. The use of a filter like plane-wave destructor enables an automatic algorithm, but leaves the option for interactive updates based on interpretation input as well. Further development of this method will help in advancing diffraction imaging technology.

Introduction

High resolution imaging of the small scale fractures in shale reservoirs improves production and recovery efficiency, reduces field development cost and decreases the environmental impact of developing the field by using fewer wells to optimally produce the reservoir. This technology is not yet deployed in the industry and is a fundamental advance in high resolution 3-D prestack data imaging of complex geological structures. Current diffraction imaging research has identified a new approach to image small scale faults, pinch-outs, salt flanks, reflector unconformities, in general any small scattering objects, by using diffraction imaging as a complement to the structural images produced by reflection imaging (Khaidukov, Landa and Moser 2004, Moser and Howard 2008, Moser 2011; see also Sturzu et al. 2013, where more references can be found). The main goal of conventional time and depth seismic processing is to enhance specular reflections. Since diffractions have a different move-out than reflections, many processing steps designed to enhance reflections, end up attenuating the diffractions. If the shale layers are thinner than half the wavelength, tuning and multiple-reverberation effects make the stratigraphic interpretation of the images difficult and unreliable. Decreasing the wavelength of the seismic waves reflected at the target is nearly impossible in surface seismic surveying because of the dissipative nature of the overburden that causes the attenuation of the high-frequency component of the seismic wave-field. Furthermore, the high frequencies that are present in the data are often lost during standard processing. Standard approaches to obtain high-resolution information, such as coherency analysis and structure-oriented filters, derive attributes from stacked, migrated images. Diffraction imaging in comparison, can act directly on the pre-stack data, and has the potential to focus and image super-resolution structural information.

Method and Theory

Diffraction imaging is the process of using diffractions to focus and image the structural elements that which are small compared to the wavelength of seismic waves. Currently, most of the algorithms that are used to process seismic data enhance reflections and suppress diffracted energy. The goal of diffraction imaging is not to replace these traditional algorithms, but rather to provide interpreters with an additional volume. Several techniques for diffraction imaging have been proposed (Khaidukov, Landa and Moser 2004, Moser and Howard 2008). They fall into two categories. In the first category are methods that separate the seismic data into two parts, one that contains the wave energy from reflections (specular energy) and the other that contains the wave energy from diffractions. Each component is used to provide an image through traditional seismic imaging methods. In the second category are methods that do not separate the input seismic data, but rather perform a filtering during migration, by attenuating or suppressing the events that satisfy to a given degree the Snell's law (Moser and Howard 2008, Moser 2009). The parameters governing this filtering are rather arbitrary without further investigation. In Sturzu et al. (2013) we introduced a new concept - specularity gathers - that proved to be very useful in the design of proper parameters for the specularity filter. Here we are showing how we can selectively filter the specular energy within specularity gathers in order to obtain the diffraction images after stacking along the specularity dimension. A conventional full wave Kirchhoff migration forms a seismic image as:

$$V(\mathbf{x}) = \int \mathrm{d}t \, \mathrm{d}\mathbf{s} \, \mathrm{d}r \, U''(t,\mathbf{s},\mathbf{r}) \, \delta\big(t - T(\mathbf{s},\mathbf{x},\mathbf{r})\big), \qquad (1)$$

where δ is the Dirac delta function, $U''(t, \mathbf{s}, \mathbf{r})$ the (second time derivative) pre-stack data, depending on time t and shot/receiver position $\mathbf{s}/\mathbf{r}$, $T(\mathbf{s}, \mathbf{x}, \mathbf{r})$ is the travel time from $\mathbf{s}$ to $\mathbf{r}$ via the subsurface image point x, computed by ray tracing in a given reference velocity model, and $V(\mathbf{x})$ the resulting migrated image. The sum is carried out over the time samples and all source and receiver pairs $(\mathbf{s}, \mathbf{r})$, in the seismic data. We define the specularity as:

$$S(\mathbf{s},\mathbf{x},\mathbf{r}) = |\boldsymbol{n}^T T_{\mathbf{x}}| / \| T_{\mathbf{x}} \|, \qquad (2)$$

where $T_{\mathbf{x}}$ denotes the gradient of $T(\mathbf{s},\mathbf{x},\mathbf{r})$ with respect to $\mathbf{x}$, and $\mathbf{n}$ is the unit vector normal to the reflector surface, depending on x as well. . For $\boldsymbol{x}$ located on a strong reflector, $S = 1$, which implies that the bisector of ray vectors from $\boldsymbol{s}$ and $\boldsymbol{r}$ is collinear with $\boldsymbol{n}$ and hence there is a pure specular reflection that has to be discarded; for $S < 1$ the energy is non-specularly scattered, which is what diffraction imaging has to enhance. Mainly because of the Fresnel-zone constraints, there is a grey zone close to $S = 1$ where the specularity filter has to be smoothly applied. A convenient way to design the specularity filter parameters that define the gray zone is to sort the migration output in specularity gathers:

$$V_{sg}(\mathbf{x}, S) = \int \mathrm{d}t\ \mathrm{d}\mathbf{s}\ \mathrm{d}\mathbf{r}\ U''(t,\mathbf{s},\mathbf{r})\ \delta\big(t - T(\mathbf{s},\mathbf{x},\mathbf{r})\big)\ \delta(S - |\mathbf{n}^T T_{\mathbf{x}}| / \| T_{\mathbf{x}} \|). \tag{3}$$

The diffraction image is obtained after a weighted stack over the specularity values:

$$V_d(\mathbf{x}) = \int_0^1 \mathrm{d}S\ \ w(\mathbf{x}, S)\ V_{sg}(\mathbf{x}, S). \tag{4}$$

This has the advantage that the weighting function is designed after migration and therefore constructed, and updated, very efficiently. In particular, the weighting function can be chosen spatially variable $w = w(\boldsymbol{x}, S)$ and adapted to the local Fresnel zone width, which is difficult to estimate a priori but becomes feasible using specularity gathers. Also, feedback from interpretation can be easily included in the weighting function, and hence in the final diffraction image. As shown in Sturzu et al. (2013), for a correct velocity model and in the high-frequency limit, a specular reflection event appears in the specularity gathers as a focused spot on the S=1-axis. Point diffractions appear as flat events extending over $0 < S < 1$. Edge diffractions in three dimensions appear as dipping events, as they obey Snell's law only along the edge, not transversely to it (Moser, 2011). Finite bandwidth reflections also appear as dipping events, as the non-specular part of reflected energy outside the Fresnel zone is not related to the shortest reflection path following Fermat's principle. However, displaying specularity gathers in the common-image option may become cumbersome; fortunately, using a common-depth display, i.e. displaying sections along one of the horizontal lines (compared to depth in the common-image case) versus specularity is able to give a much clear image (Figure 2). In the common-depth display, the specular reflections are almost horizontal events having the extension of the reflectors. An important issue is that in this display one can identify (out Fresnel zone –) ghosts of the specular events coming from lower depths, which are almost horizontal events as well. In this way we can filter these events together with their "primaries."

A workflow for diffraction imaging using common-depth specularity gathers consists of: I. Standard pre-stack depth migration using formula (1) and associated migration velocity analysis to obtain an optimally focused full-wave image $V(\mathbf{x})$; II. Extraction of unit vector normal to the reflector surface using $V(\mathbf{x})$ each point $\mathbf{x}$; III Migrating using formula (3) to obtain a specularity gather; IV Filtering the specular energy from the specularity gather; V Stacking over specularity dimension to obtain a diffraction image.

Examples

The Kirchhoff migrations are performed using Z-Terra's pre-stack depth migration program ZTK, in which the diffraction imaging method was implemented through the procedure outlined above (Eqs. 1-3). The first example (Figure 1) illustrates the functionality of specularity gathers on a simple diffraction ramp model. The specularity gather of Figure 1a shows horizontal events close to S = 1 for specular reflections shown in the stack from Figure 1b at 1400 m in depth, while for diffractive events from the same depth at 750 m, 1500 m, and 2250 m along the line, we notice clearly defined peaks. We used a plane wave-destructor filter (PWD) as described in Fomel (2002) to attenuate the specular energy, and the result is displayed in Figure 2c. Stacking over the values of specularity lower than 0.97 gives the diffraction image from Figure 1d.

The second example is the Mare di Cassis data set (Moser and Howard, 2008). Figure 2 shows a comparison between a specularity gather in common-depth display (CDSG) and one in common-image display. In Figure 3 the result of applying the PWD filter on CDSG is shown for a depth section at 1310 m. Figure 4 displays the standard migration image and the diffraction image obtained by stacking over specularities smaller than 0.97 of the PWD filtered CDSG.

The third example concerns a production dataset from the Kenedy-Eagle Ford shale play (Texas). Here diffraction imaging has been carried out in the framework of a full 3D depth imaging process. Figures 5 and 6 show the results for a depth slice at 4790 m. In this case, due to the 3D geometry, the diffraction peaks from the CDSG are less pronounced than in the synthetic examples. However, by applying the procedure described above one is able to delineate in the migration image (Figure 6c) diffractive formation like narrow channels (the cutouts have not been part of the survey).

Conclusions

In this paper, we introduced a method to filter the specular energy from specularity gathers in order to obtain diffraction images. The use of a filter like plane-wave destructor enables an automatic algorithm, but leaves the option for interactive updates based on interpretation input as well. Further development of this method will help in advancing diffraction imaging technology.

Acknowledgements

We thank Marathon Oil and Seitel for permission to show the Eagle Ford data, and Opera (Pau) for providing the Mare di Cassis data set.

References

Fomel, S., 2002. Applications of plane-wave destruction filters, Geophysics, 67, 1946-1960.

Khaidukov V., Landa E. and Moser T.J., 2004. Diffraction imaging by focusing-defocusing: An outlook on seismic superresolution. Geophysics 69, 1478–1490.

Moser T.J. and Howard, C.B. 2008. Diffraction imaging in depth, Geophysical Prospecting 56, 627.

Moser T.J., 2011. Edge and Tip Diffraction Imaging in Three Dimensions, 73rd EAGE Conference Vienna, Extended Abstracts.

Sturzu I., Popovici A.M., Tanushev N., Musat, I., Pelissier M.A. and Moser T.J., 2013. Specularity Gathers for Diffraction Imaging, 75th EAGE Conference, London, England, Expanded Abstracts.

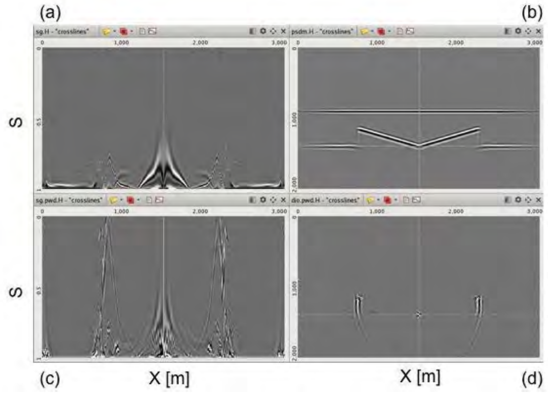

Figure 1: Diffraction ramp model: (a) Specularity gather in common-depth display for 1400 m. (b) Standard migration image obtained by stacking over specularity of the specularity gather (a). (c) Specularity gather in common-depth display for 1400 m filtered with PWD. (d) Diffraction image obtained by stacking over specularity of the PWD filtered specularity gather (c).

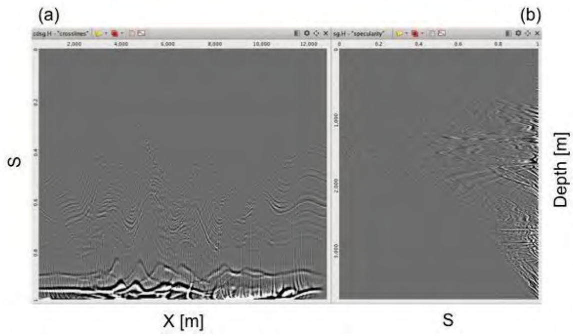

Figure 2: Mare di Cassis model: (a) Specularity gather in common-depth display for 2100 m. (b) Specularity gather in common-image display for x=4880 m.

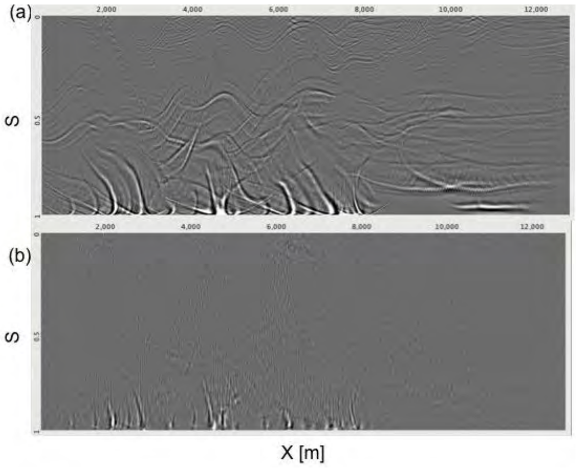

Figure 3: *Mare di Cassis model: (a) Common-Depth Specularity Gather (CDSG) for 1310 m. (b) PWD filtered CDSG 1310 m.*

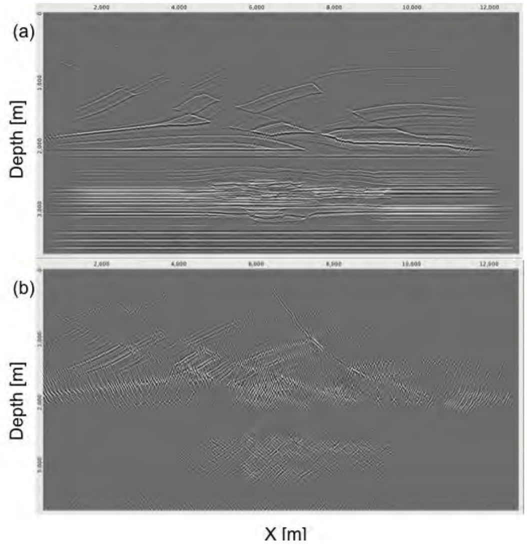

Figure 4: *Mare di Cassis model: (a) Standard migration image (b) Diffraction image obtained by stacking over specularity of the PWD filtered specularity gather.*

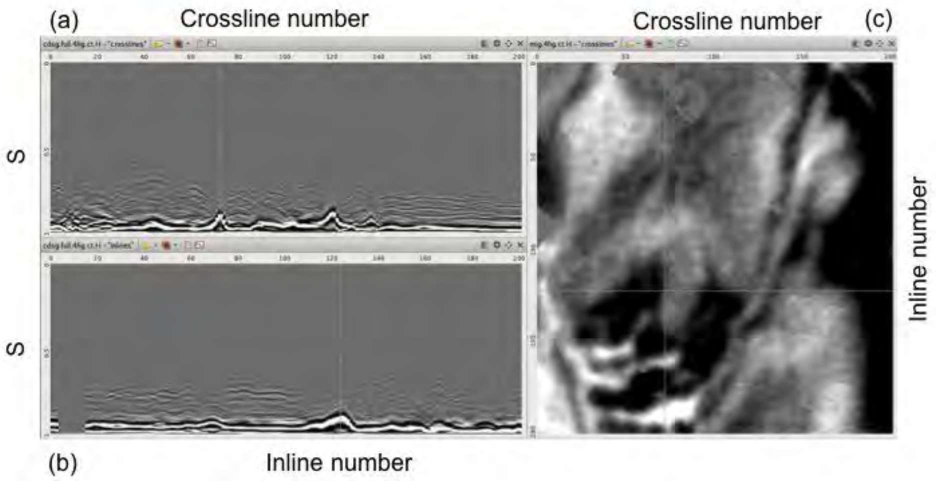

Figure 5: *Migration result for the Eagle Ford dataset at 4790 m: CDSG along (a) inline 123 (b) crossline 72 (c) Standard migration image..*

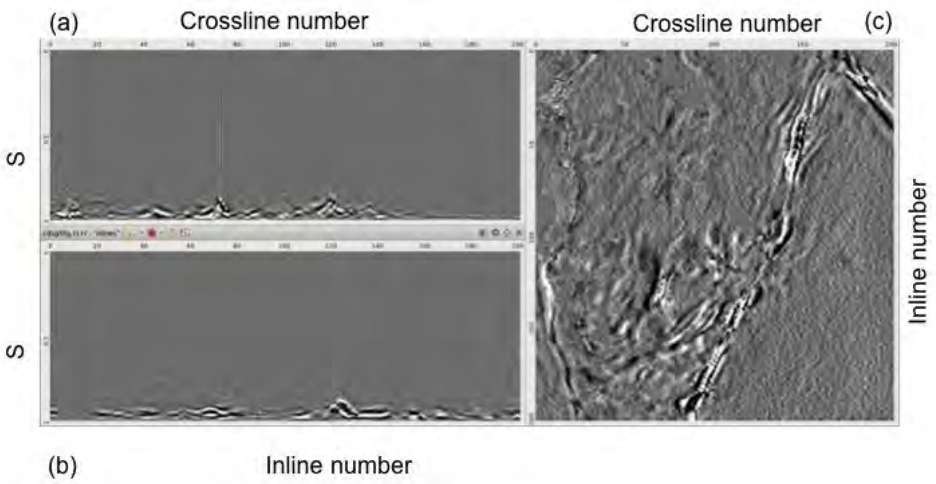

Figure 6: *Migration result for the Eagle Ford dataset at 4790 m: PWD filtered CDSG along (a) inline 123. (b) crossline 72. (c) Diffraction image.*